# 5.3 THE MICROPHYSICAL PROCESSES OF TYPHOON NARI (2001) AT LANDFALL

Ming-Jen Yang
National Central University, Chung-Li, Taiwan

## 1. INTRODUCTION

Typhoon Nari struck Taiwan on September 16, 2001; it brought heavy rainfall, fresh flood, and caused severe economical and societal damage, including 92 human lives (Sui et al. 2002). The first objective of this study is to investigate whether the model can reproduce the track, intensity, kinematic, and precipitation features of Typhoon Nari during its landfall on Taiwan from the given subtropical synoptic conditions, as verified against satellite, rain gauge, and radar observations. The second purpose is to examine the essential microphysical processes responsible of heavy rainfall associated with the landfalling storm. The third objective is to investigate the sensitivity of simulated storm's track, intensity, and precipitation structures to the microphysics parameterization schemes used in the model. Through a series of microphysics sensitivity experiments, we wish to gain insight into the relative importance of different microphysical processes in generating Nari's heavy rainfall over Taiwan.

## 2. METHODOLOGY

The PSU-NCAR MM5 model (Grell et al. 1995) is used to simulate Typhoon Nari (2001). The MM5 model configuration includes four nested grids with horizontal grid size of 54, 18, 6, and 2 km,respectively. The simulation is integrated for 84 h, starting from 120 UTC 15 September 2001. The initial and boundary conditions are taken from the ECMWF advanced global analysis with $1.125^{o}$ x $1.125^{o}$ horizontal resolution. The following physics options are used in the control (CTL) simulation: the Grell (1993) cumulus parameterization scheme, the Reisner microphysics scheme with graupel (Reisner et al. 1998), the MRF PBL scheme (Hong and Pan 1996), and the atmospheric radiation scheme of Dudhia (1989). Note that no cumulus parameterization scheme is used on the 6 and 2-km grids. Details in the model setup can be found in Yang and Huang (2006) and Yang et al. (2007). Precipitation efficiency of Typhoon Nari over the ocean was discussed in Sui et al. (2005), and the flooding simulation of Nari was examined in Li et al. (2005).

*Corresponding author address: Prof. Ming-Jen Yang, Institute of Hydrological Sciences, National Central University, Chung-Li, 320, Taiwan. E-mail: mingjen@cc.ncu.edu.tw

Liu et al. (1997) was the first to obtain a successful real-data explicit simulation of a TC, i.e., Hurricane Andrew (1992), using the PSU-NCAR MM5 model. The model reproduces well the hurricane track, intensity and intensity change as well as the radius of maximum winds (RMW), the hurricane eye/eyewall, and the spiral rainbands. In this study, we wish to extend the kind of TC modeling studies by conducting a cloud-resolving simulation of Typhoon Nari (2001) occurring over the Northwest Pacific, but we will focus more on its precipitation features, particularly the microphysical effects, as Nari moves across Taiwan.

Yang and Houze (1995) indicated that the simulated dynamic and kinematic features, such as rear inflow, of a squall-line type mesoscale convective system are highly sensitive to the microphysical parameterization scheme employed in the model. Wang (2002) further showed in his idealized TC simulations that the cloud structures of the simulated TC are quite sensitive to the cloud microphysics scheme; however, the intensification rate and the final intensity are not sensitive to the details of cloud microphysics parameterizations. From a series of 5-day simulation of Hurricane Bonnie (1998), Zhu and Zhang (2006) pointed out that varying cloud microphysical processes produce little sensitivity in TC's track, but different microphysics schemes generate pronounced departures in TC's intensity and inner-core structures.

To understand the impact of microphysics parameterization on the simulated Nari's track and precipitation structure, four numerical sensitivity experiments are conducted in this study (Table 1). The model setup and physical options of the sensitivity experiments, except for the tested microphysics scheme, are the same as those in the CTL run. WARM experiment only allows warm-rain processes; in other words, no ice-phase processes are considered in the model. NEVP run is similar to the CTL run, except for no evaporation of raindrops. NMLT experiment does not permit melting of snowflakes and graupels when environmental temperature is warmer than $0^{o}$C. Similarly, NSUB experiment does not allow sublimation of snowflakes and graupels at upper levels in the subsaturated environment as temperature is below $0^{o}$C,

## 3. RESULTS

Figure 1 compares the model-simulated track of Nari from the CTL run to the CWB best-track estimates, using results from the 6-km, larger-area covered domain. In general, the MM5 simulates very well Nari's track, especially its landfall near Yilan at 22 h into the integration (valid at 1000 UTC 16 September, henceforth 16/10), albeit 3 h earlier than and 20 km to the north of the observed. The model also reproduces reasonably well the relatively fast and slow passage of Nari from northeast to southwest across Taiwan before and after 17/00, respectively. However, the simulated track begins to deviate from the observed after 18/12, leading to large displacement errors at the end of the 84-h integration.

Figure 2a shows the simulated low-level radar reflectivity field of the CTL run at 0300 UTC 16 September when Nari was still over the ocean, and Fig. 2b displays the radar reflectivity features at 1500 UTC 16 September when Nari already made landfall. It is clear that before landfall, Nari's precipitation feature was very axis-symmetric; after landfall, Taiwan's terrain induced asymmetric pattern on the precipitation field, with enhanced rainfall on the windward slopes and mountain peaks. The simulated hydrometer fields of the CTL run before and after landfall are shown in Figs 2c, and 2d, respectively. Before landfall, snowflakes occurred in upper levels, and heavier graupel particles are mostly confined within the eyewall and spiral rainbands. Raindrops are located at low levels (below the $0^{o}$C isotherm), mainly produced by the melting of graupel particles. The vertical distribution of hydrometer fields after landfall is similar to that before landfall, except for the fact that there are less snowflakes and graupel particles at upper level, owing to weaker updrafts and convection after Nari's landfall on Taiwan. On the other hand, there is more precipitation (in the form of raindrop) along the mountain slopes, as a result of rapid saturation as the moisture-rich airflows ascending over Taiwan's rugged terrain.

Figure 3 illustrates the simulated tracks of four microphysics sensitivity experiments. It is clear from Fig. 3 that for the first 2 days (0000 UTC 16 September to 0000 18 September), varying microphysics parameterization does not have a significant impact on the simulated Nari's track, consistent with Zhu and Zhang (2006). The simulated tracks began to have substantial variations on the third and fourth days. Time series of sea-level pressure and surface maximum wind for four sensitivity experiments and the CTL run are shown in Fig.4. Without the ice-phase latent heating/cooling processes (depositional warming and sublimative cooling), the WARM experiment produced the weakest storm in both sea-level pressure and surface maximum wind in the landfall period. In the first 12 hours (1200 UTC 16 September to 0000 UTC 17 September) during the landfall period, NEVP and NMLT experiments had stronger intensities compared to WARM and NSUB experiments. One day after landfall (i.e., after 0000 UTC 17 September), storm intensities in four sensitivity experiments are very similar, and it is difficult to choose a storm persistently stronger than other storms.

Horizontal cross sections of low-level radar reflectivity fields of four microphysics sensitivity experiments are displayed in Fig. 5, and the corresponding vertical hydrometeors are shown in Fig. 6. For WARM experiment, raindrops are all confined within the eyewall, and there are no spiral rainbands (Figs. 5a and 6a), which is consistent with Wang (2002) and Zhu and Zhang (2006). Without the evaporation of raindrops, NEVP experiment showed more surface rainfall on Taiwan (Figs. 5b and 6b). Without the melting of graupels and snowflakes, NMLT storm produced less rainfall (Figs. 5c and 6c), compared to the CTL run and NEVP experiment. In the absence of sublimation of snowflakes and graupels, NSUB experiments generated more snowflakes at upper levels, which resulted in more surface rainfall through the melting of snowflakes and graupels (Figs. 5d and 6d). More details of the sensitivity experiments will be presented in the conference.

## Reference


Dudhia, J. 1989: Numerical simulation of convection observed during the Winter Monsoon Experiment using a mesoscale two-dimensional model. *J. Atmos. Sci*., **46**, 3077-3107.

Grell, G. A., 1993: Prognostic evaluation of assumptions used by cumulus parameterizations. *Mon. Wea. Rev*., **121**, 764-787.

Grell, G. A., J. Dudhia, and D.R.Stauffer,1995: A description of the fifth-generation Penn State/NCAR Mesoscale Model. NCAR Technical Note,122 pp.

Hong, S.-Y., and H.-L. Pan, 1996: Nocturnal boundary layer vertical diffusion in a medium-range forecast model. *Mon. Wea. Rev.*, **124**, 2322-2339.

Li, M.-H., M.-J. Yang, R. Soong, and H.-L. Huang**,** 2005: Simulating typhoon floods with gauge data and mesoscale modeled rainfall in a mountainous watershed. *J. Hydrometeor*., **6**, 306–323.

Liu, Y., D.-L. Zhang, and M. K. Yau, 1997: A multiscale numerical study of Hurricane Andrew (1992). Part I: Explicit simulation and verification. *Mon. Wea. Rev.*, **125**, 3073–3093.

Reisner, J., R. J. Rasmussen, and R. T. Bruitjes, 1998: Explicit forecasting of supercooled liquid water in winter storms using the MM5 mesoscaled model. *Quart. J. Roy. Meteor. Soc.*, **124**, 1071-1107.

Sui, C.-H., C.-Y. Huang, Y.-B. Tsai, C.-S. Chen, P.-L. Lin, S.-L. Shieh, M.-H. Li, Y.-A. Liou, T.-C. C. Wang, R.-S. Wu, G.-R. Liou, Y.-H. Chu, 2002: Typhoon Nari and Taipei flood—A pilot meteorology-hydrology study. EOS, Transctions, *Amer. Geophy. Union*, **83**,

265, 268–270.

Sui, C.-H., X. Li, M.-J. Yang, and H.-L. Huang**,** 2005: Estimation of oceanic precipitation efficiency in cloud models. *J. Atmos. Sci.*, **62**, 4358–4370.

Wang, Y., 2002: An explicit simulation of tropical cyclones with a triply nested movable mesh primitive equation model: TCM3. Part II: Model refinements and sensitivity to cloud microphysics parameterization. *Mon. Wea. Rev.*, **130**, 3022–3036.

Yang, M.-J., and R. A. Houze, Jr., 1995: Sensitivity of squall-line rear inflow to ice microphysics and environmental humidity. *Mon. Wea. Rev*., **123**, 3175-3193.

Yang, M.-J., and H.-L. Huang, 2006: A Modeling Study of Typhoon Nari (2001): Verification and topographic effects. *Preprints, The 27th Conference on Hurricanes and Tropical Meteorology*, Monterey Bay, CA, 24-28 April 2006, Amer. Meteor. Soc.

Yang, M.-J., H.-L. Huang, and D.-L. Zhang, 2007: A modeling study of Typhoon Nari (2001) at landfall. Part I: The topographic effects. *J. Atmos. Sci.*, revised.

Zhu, T., and D.-L. Zhang, 2006: Numerical simulation of Hurricane Bonnie (1998). Part II: Sensitivity to cloud microphysical processes. *J. Atmos. Sci*, **63**, 109-126.

Table 1: Microphysics sensitivity experiments.

| Experiment | Description |
|---|---|
| WARM | Warm rain processes only |
| NEVP | No evaporation of raindrops |
| NMLT | No melting of snowflakes and graupels |
| NSUB | No sublimation of snowflakes and graupels |

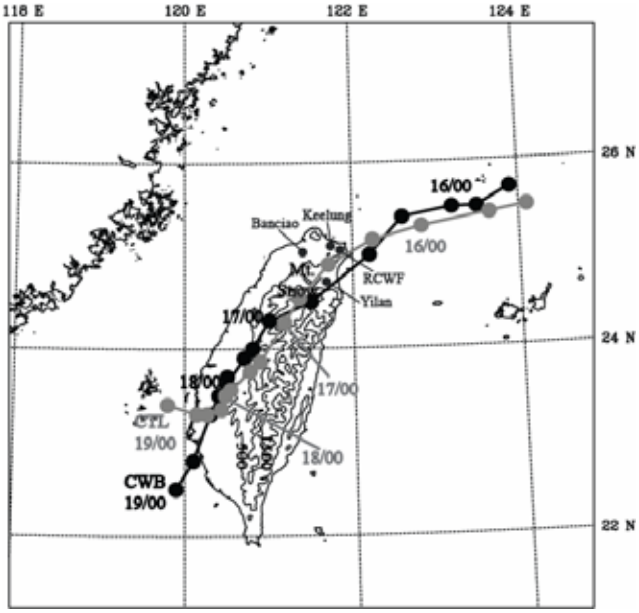


Figure 1: Comparison of the CWB best track (CWB; thick solid) and the simulated track (CTL; grey solid) of Typhoon Nari, superposed with the terrain height (thin solid) at 1000-m intervals (starting

at 500-m height). Each dot denotes Nari's central position every 6 h. The inset table is for the simulated track error with respect to the CWB analysis at 12 hourly intervals.

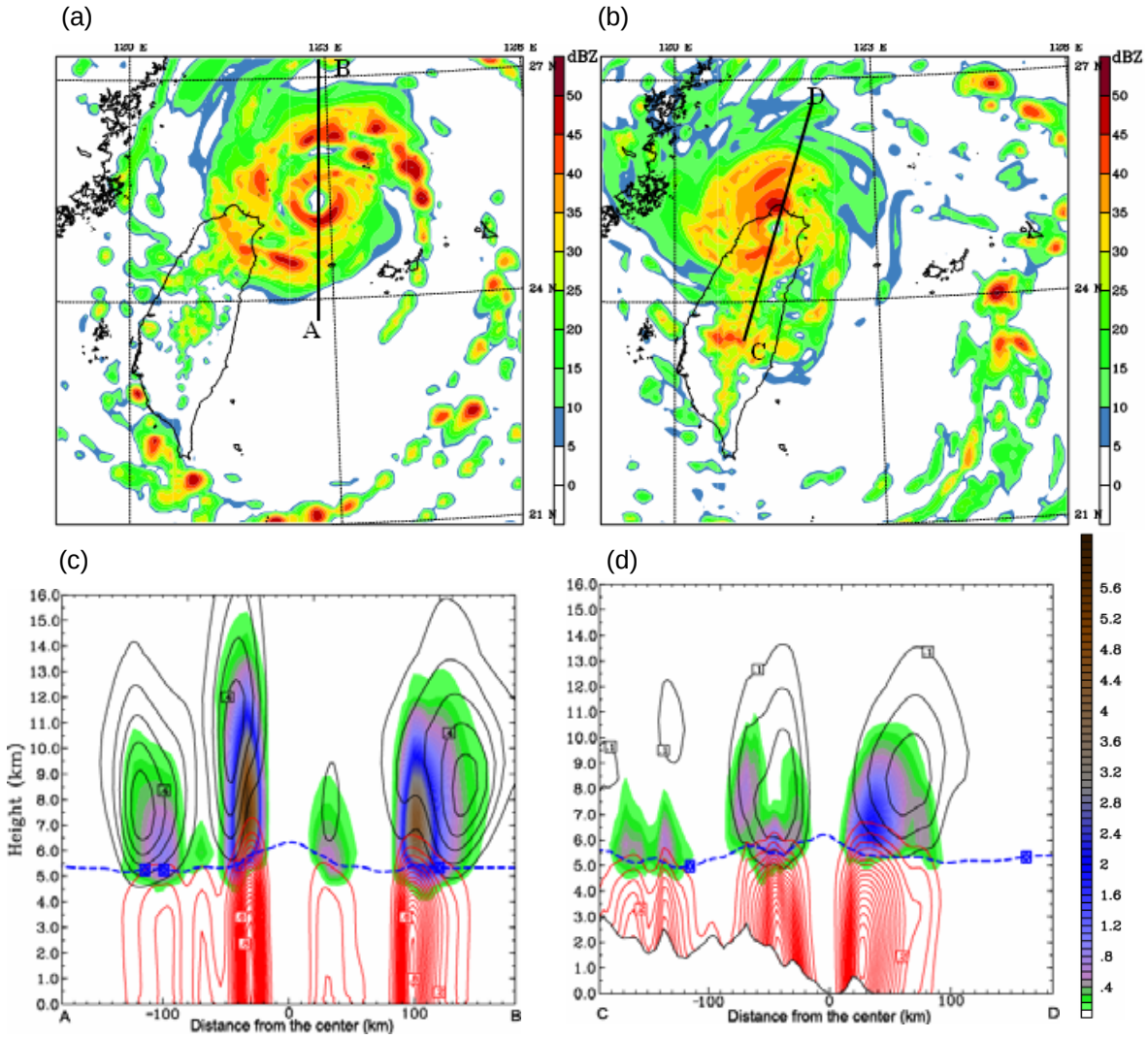


Figure 2: Horizontal cross sections of simulated low-level radar reflectivity field (in dBZ) at a) 0300 UTC 16 September, and b) 1500 UTC 16 September 2001, and the vertical cross sections of simulated mixing ratio field (in g/kg) of snowflake (in black contour), rain water (in red contour), and graupel (colored) along the AB line at c) 0300 UTC 16 September and along the CD line at d) 1500 UTC 16 September 2001. The blue dashed line is the 0$^{o}$C isotherm.

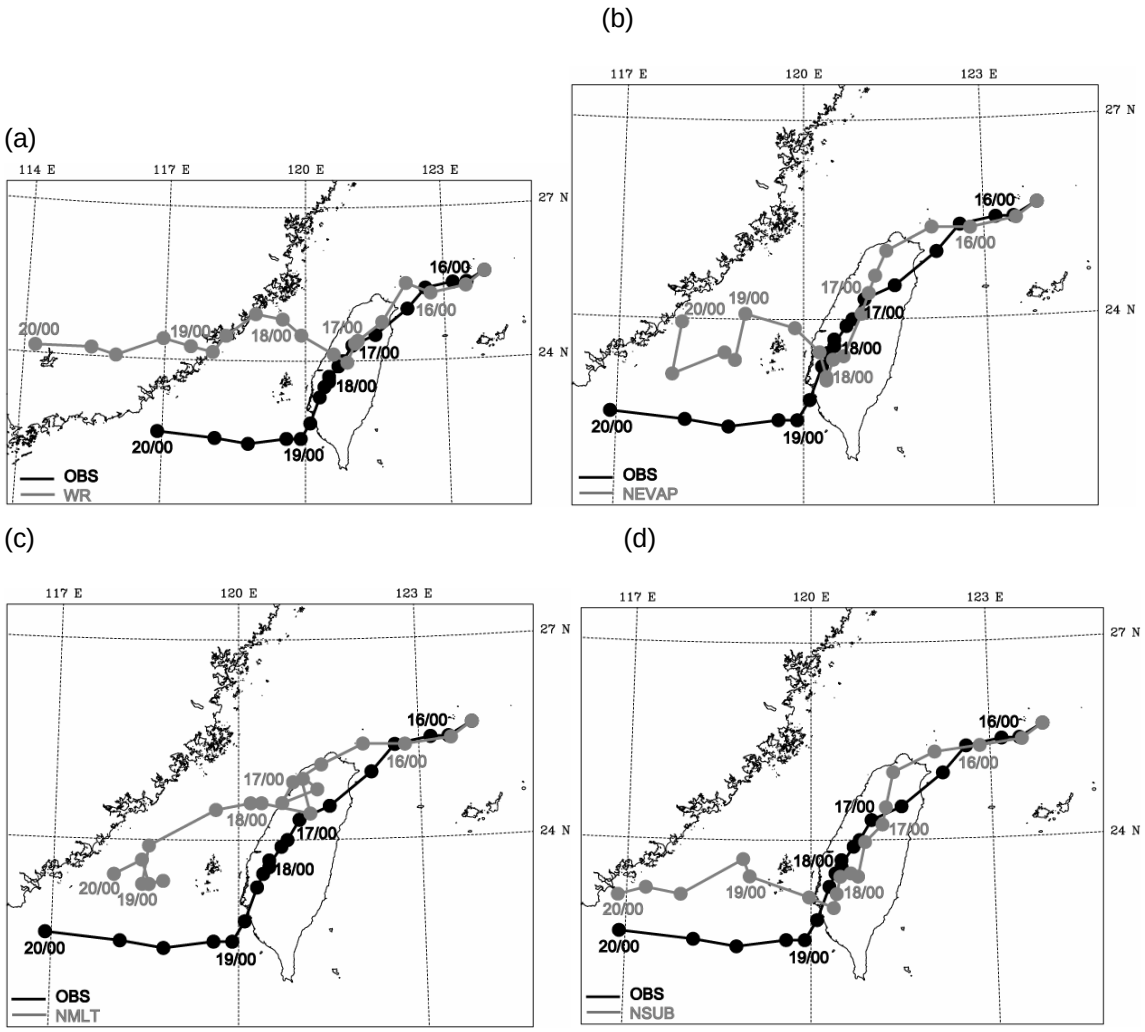


Figure 3: Simulated Nari tracks of the (a) WARM, (b) NEVP, (c) NMLT, and (d) NSUB experiments. The observed track from the CWB best-track analysis is also shown for comparison.

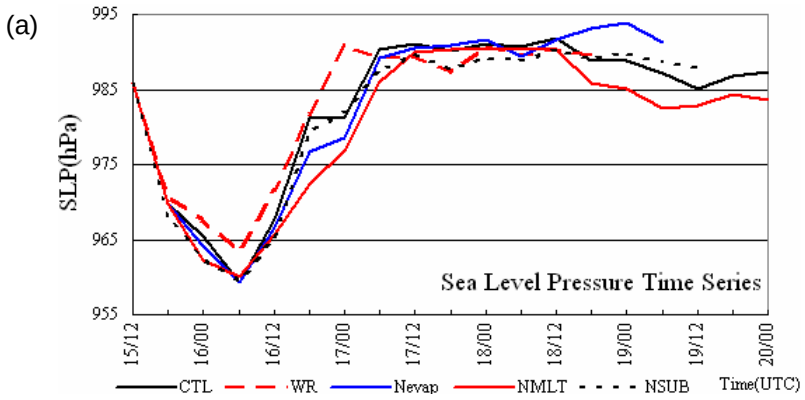

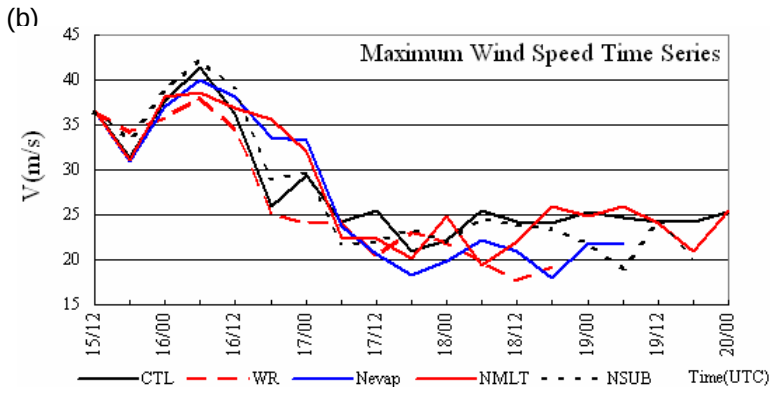


Figure 4: Time series of (a) sea-level pressure (SLP), and (b) near-surface maximum wind (V) from the control (CTL) and microphysics sensitivity experiments.

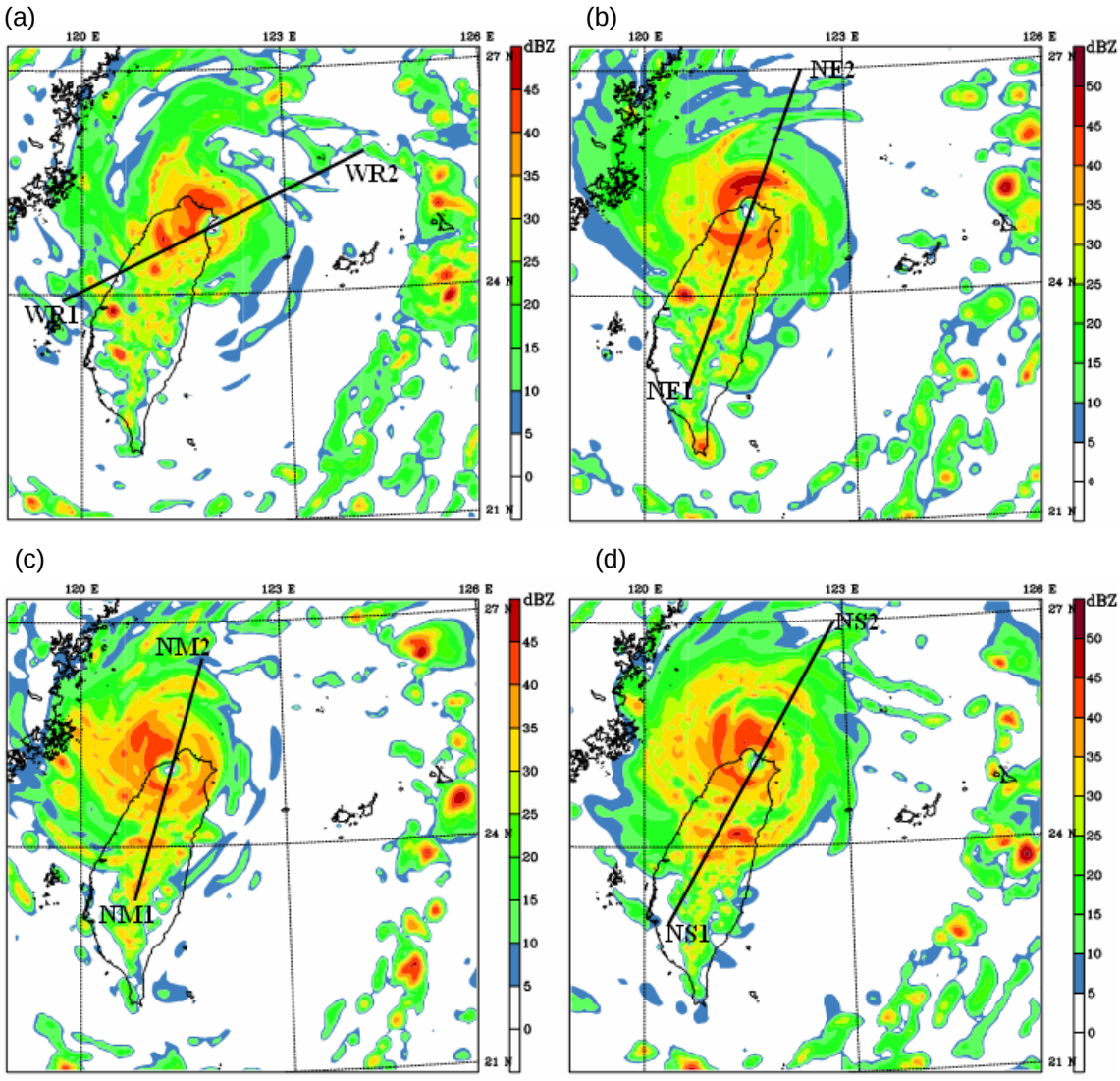

Figure 5: Horizontal cross sections of simulated radar reflectivity fields of the (a) WARM, (b) NEVP, (c) NMLT, and (d) NSUB experiments when the simulated Typhoon Nari made landfall. Lines WR1–WR2, NE1–NE2, NM1–NM2, NS1–NS2 denotes the horizontal location of vertical cross sections used in Figs. 6a (WARM experiment), 6b (NEVP experiment), 6c (NMLT experiment), and 6d (NSUB experiment), respectively.

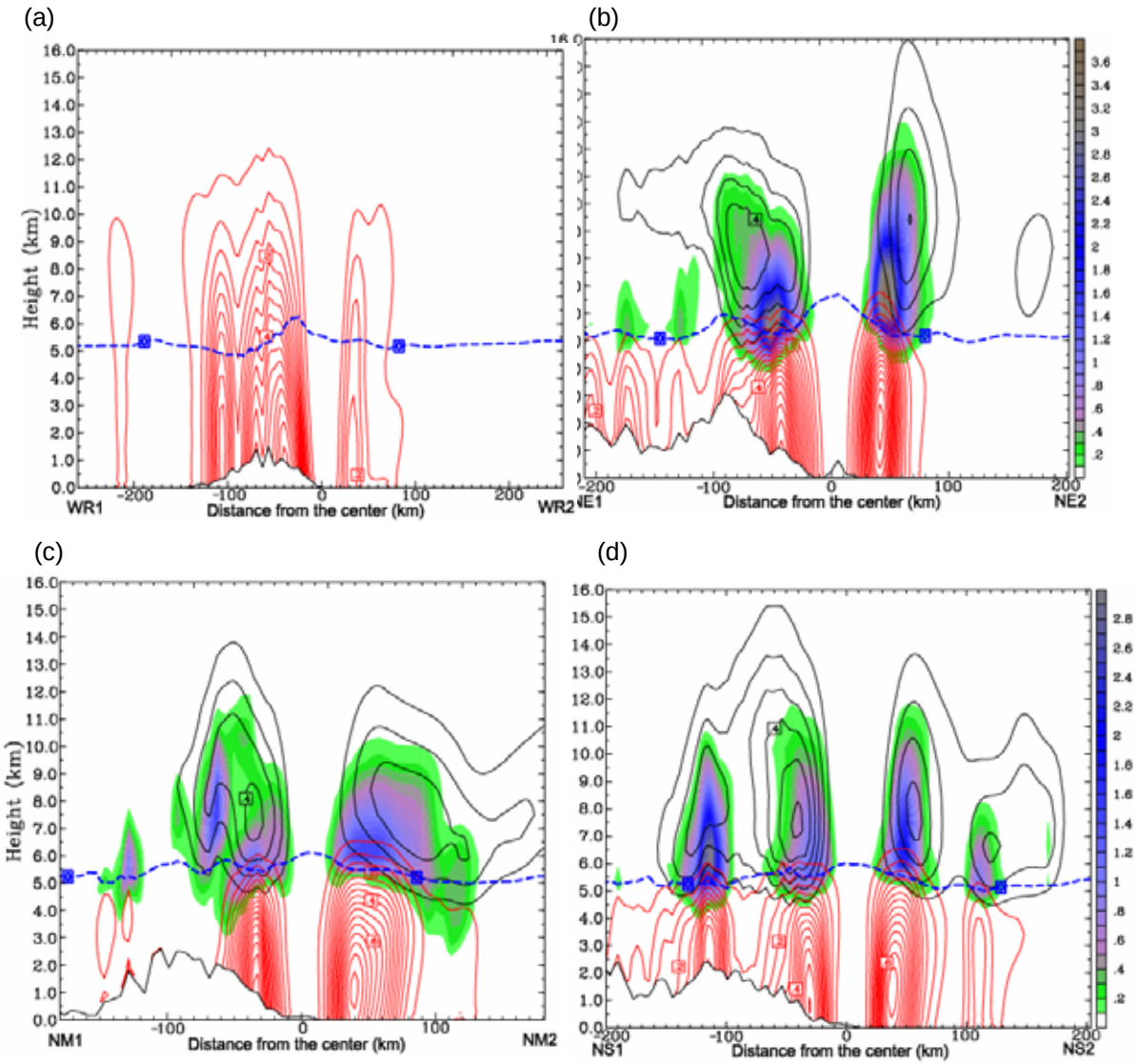


Figure 6: Vertical cross sections of simulated mixing ratio fields of snowflake (in black contour), rain water (in red contour), and graupel (colored) of the (a) WARM, (b) NEVP, (c) NMLT, and (d) NSUB experiments across Taiwan's Central Mountain Range when the simulated Typhoon Nari made landfall. The horizontal locations of vertical cross sections WR1–WR2, NE1–NE2, NM1–NM2, NS1–NS2 are shown in Figs. 5a, 5b, 5c, and 5d, respectively.